Design Proposal – Mach-Zehnder Interferometer

SEAN O'CONNOR

The Johns Hopkins University Applied Physics Laboratory, Laurel, MD
sean.oconnor@jhuapl.edu

Abstract: This report describes the theory, design, and fabrication of a range of unbalanced Mach-Zehnder interferometers on a silicon photonic integrated circuit process. The goal is to extract the optical waveguide group index from the interferometer experimental results and compare it to the value obtained from simulation results. A Michelson interferometer will also be fabricated at one length offset for comparison to the Mach-Zehnder structure.

1. Introduction

Mach-Zehnder interferometers (MZIs) and Michelson interferometers are powerful optical structures that can be used electro-optic modulation, optical switches, filters, and various optical sensors. They can translate small perturbations of optical phase into amplitude perturbations which are more easily measured. In this report, multiple iterations of an unbalanced MZI will be designed and realized on a silicon photonic integrated circuit (PIC). The length imbalances that will be fabricated will be in the range of 25-125um in 25um steps for a total of five different MZI structures. The group index of the silicon optical waveguide will be extracted from the measured results and compared to the simulated values. In addition, a Michelson interferometer with a length imbalance of 50um will be fabricated for comparison purposes.

2. Theory

A basic MZI is shown in Fig. 1. It consists of two y-branch splitters; one to split the light from the optical source and one to recombine the two paths for optical detection. Between the y-branch splitters there are two lengths of optical waveguide with lengths *L1* and *L2*.

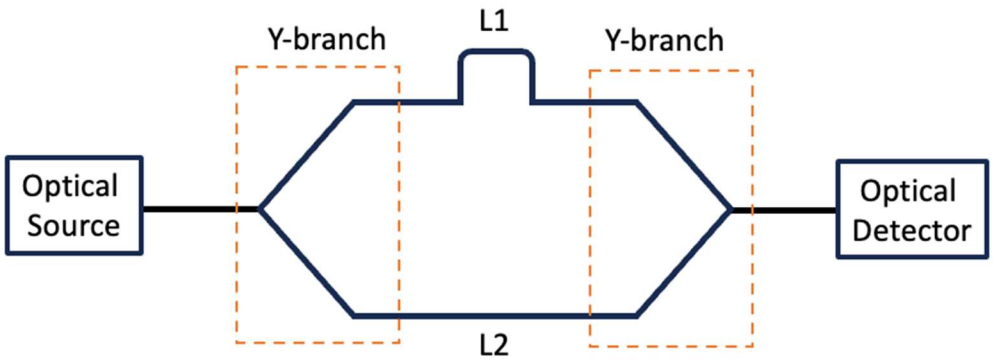

Figure 1: A basic MZI structure shown with L1 ≠ L2

If $L1 = L2$, the MZI is considered to be balanced with an output intensity *(Io)* represented by the following equation [1]:

$$Io = \frac{Ii}{2}[1 + \cos(\Delta\beta L)] \,. \quad (1)$$

The output intensity, as seen in (1), is dependent on the input intensity *(Ii)* and is sinusoidally varying with the difference in the propagation constants (β) between the arms. The propagation constant, β, is equal to $2\pi n/\lambda_0$ where n is the effective index of the waveguide and λ_0 is the wavelength if operation. The waveguide length (L) is a constant since we have defined $L1 = L2$. It is important to note that (1) refers to a balanced MZI that is lossless. Changes in propagation constant of a silicon optical waveguide can be realized by modifying the refractive index of the waveguide via temperature or carrier injection. These are the primary methods used in thermo-optic switches and high-speed electro-optic modulators.

The optical output intensity of a lossless unbalanced MZI (i.e. $L1 \neq L2$) can be represented by the following equation [1]:

$$Io = \frac{Ii}{2}[1 + \cos(\beta \Delta L)] \; . \quad (2)$$

In (2), the propagation constants of the two waveguides are constant but vary in their respectively lengths. This is the structure this report will focus on.

An alternative to the MZI is a Michelson interferometer. This structure is shown in Figure 2. The Michelson interferometer uses a 2x2 coupler, two optical waveguides, and two loop mirrors. The optical signal is input into the top port of the 2x2 coupler and split equally onto the two output paths. The signal propagates through the two optical waveguides, bounces off the loop mirror, and propagates back to the 2x2 coupler. If $L1 \neq L2$ then the Michelson interferometer will have a similar transfer function as the MZI. However, the difference in length between $L1$ and $L2$ is counted twice since the signal propagates through both of the waveguides in the forward and reverse direction.

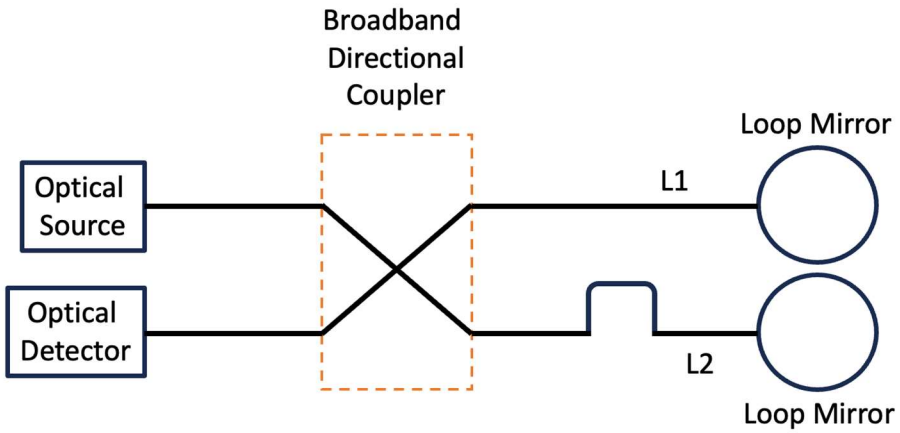

Figure 2: Michelson Interferometer

3. Modeling and simulation

3.1 Waveguide Modeling

Key to understanding the MZI is the optical waveguides that make up the structure. These waveguides are made of silicon surrounded with silicon dioxide (SiO_2). The refractive index difference between the two materials allows a guided optical wave in the silicon waveguide. The waveguides of interest are 220nm thick and 500nm wide. This geometry only supports one transverse electric (TE) mode and one transverse magnetic (TM) mode. We will be focused

on the TE mode for this report. Figure 3 shows a cross section of the mode profile of the TE1 mode excited with 1550nm light obtained the software package Lumerical MODE.

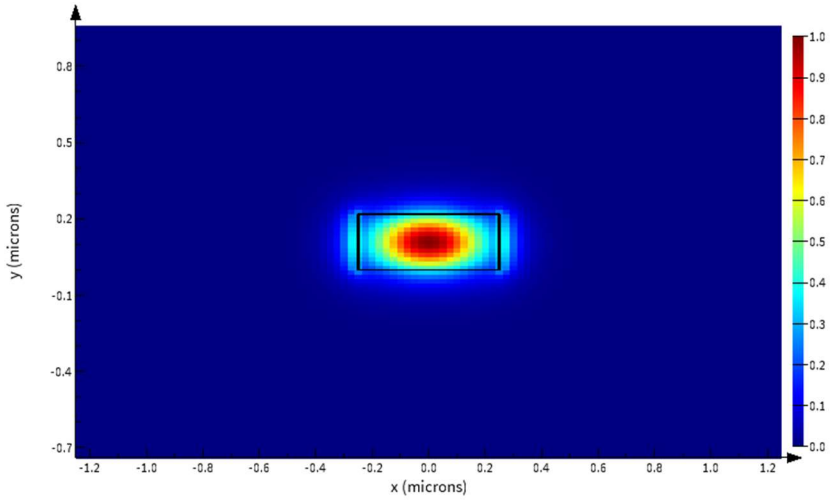

Figure 3: Mode profile of TE1 mode for a 220nm x 500nm silicon waveguide

It can be seen that the mode is well confined in the silicon waveguide. As part of the waveguide simulations, the effective and group index can be extracted. These values are important to the design of a MZI because they define how fast or slow light propagates in the waveguide. Figure 4 shows both the effective and group index of a silicon waveguide at different incident wavelengths.

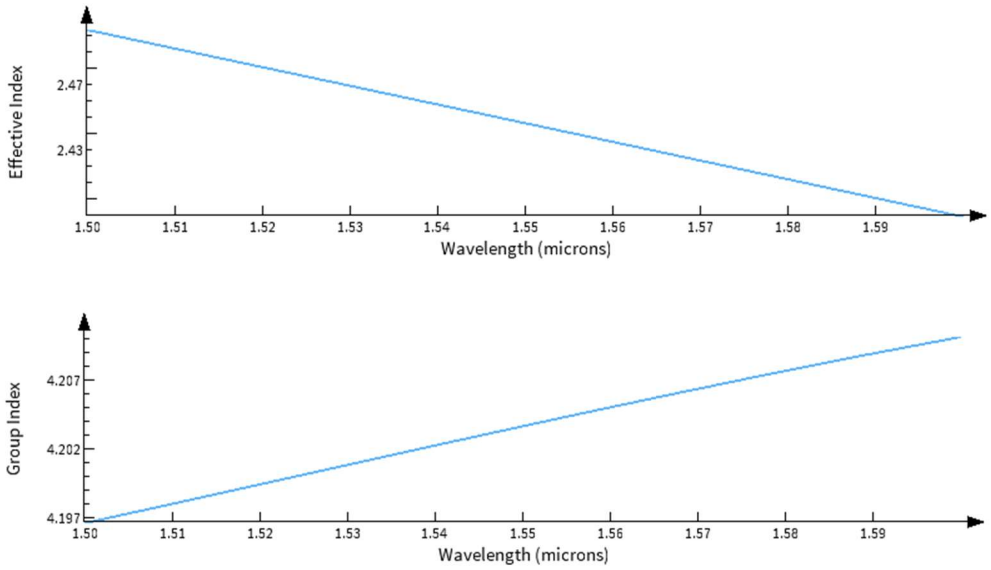

Figure 4: Wavelength dependence of effective and group index of 220nm x 500nm silicon waveguide

As wavelength increases, the effective index decreases and the group index increases. At 1550nm, the effective index is ~2.44 and the group index is ~4.2.

When modeling complex photonic structures, it can be useful to have a compact model for optical waveguides. A compact model describes the behavior of the optical waveguide with an

equation. In this case, we are interested to modeling the effective index with wavelength. The expression used for a 220nm x 500nm silicon waveguide is the following [1]:

$$neff(\lambda) = n_1 + n_2(\lambda - \lambda_0) + n_3(\lambda - \lambda_0)^2 \,. \qquad (3)$$

Using a wavelength of 1550nm (i.e. λ_0 = 1550e-9), n_1 = 2.44, n_2 = -1.133, and n_3 = -0.0439. This result was achieved by curve fitting the effective index versus wavelength simulation data obtained from Lumerical MODE.

3.2 MZI Modeling

Knowing how the effective and group index behave with wavelength is crucial to modeling the more complex MZI structure. As seen in (1) and (2), the MZI transfer function has a wavelength dependence via the propagation constant, β. The MZI response will sinusoidally vary with wavelength and the distance in nanometers between one peak of the transfer function and the adjacent peak is called the free spectral range (FSR). A small FSR will have many peaks per nanometer of incident wavelength and a large FSR will have few. This single value allows for intuitive understanding of the MZI transfer function. For the report we will evaluating how length differences in the two MZI arms effect the FSR of the MZI. Table 1 shows the planned length variations and the expected FSR values. The FSR values in Table 1 were obtained with Lumerical INTERCONNECT simulation software.

Table 1: FSR with different length offsets at 1550nm

Length offset (um)	Free Spectral Range (nm)
25	21.61
50	11.34
75	7.48
100	5.68
125	4.59

The Lumerical INTERCONNECT circuit diagram that yielded the results in Table 1 is shown in Figure 4. In this circuit diagram we have an optical network analyzer (*ONA_1*) to stimulate and record the transfer function of the MZI. The circuit itself is comprised of a grating coupler s-parameter block (*SPAR_3* and *SPAR_4*), a y-branch splitter s-parameter block (*SPAR_1* and *SPAR_2*), and two waveguide blocks (*WGD_1* and *WGD_2*).

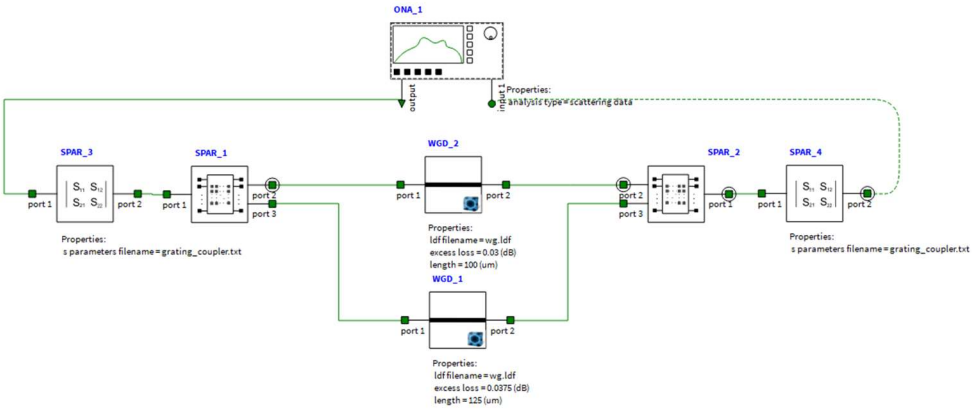

Figure 5: Lumerical INTERCONNECT circuit diagram of a MZI

A graph of the transmission of the MZI represented in Figure 5 is shown in Figure 6. Here one can see the output sinusoidally varying with increasing wavelength.

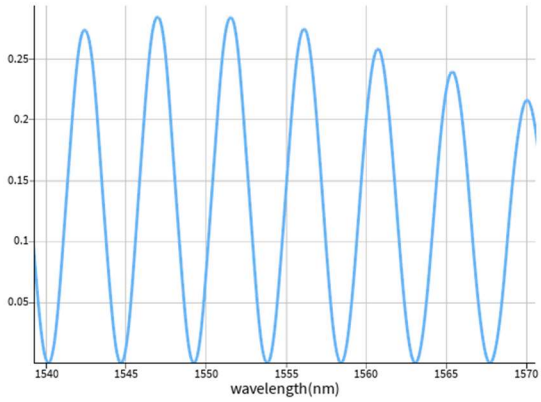

Figure 6: Transmission of an unbalanced MZI

The length offset between MZI arms in Figure 5 was 125um yielding a free spectral range of roughly 5nm.

The group index of the waveguides and can found from measuring the FSR of an unbalanced MZI. The peaks of the transfer function (2) occur when the argument of the cosine term is equal to a multiple of 2π. Using this knowledge, with some approximations, one can arrive at the following equation relating FSR to group index [1]:

$$FSR = \frac{\lambda^2}{\Delta L n_g}. \qquad (4)$$

For example, using the FSR predicted in Table 1 for 125um length offset at 1550nm, the group index can be calculated to be 4.18. This is in agreement with the plots shown in Figure 3. This same approach will be used to calculate the group index of the fabricated waveguides from the measured data.

3.3 Michelson Interferometer Modeling

The Michelson interferometer circuit diagram is shown in Figure 7.

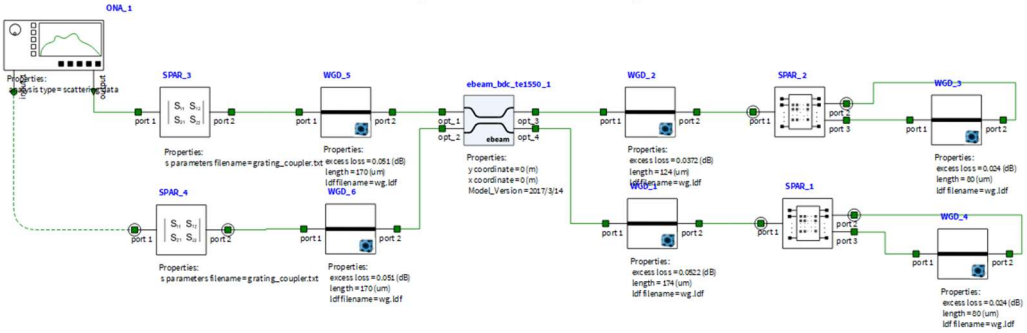

Figure 7: Michelson interferometer circuit diagram using Lumerical INTERCONNECT

This circuit diagram uses similar blocks to the MZI circuit including the optical network analyzer, grating coupler s-parameter blocks, y-branches, and optical waveguides. The new block is the broadband 2x2 coupler (*ebeam_bds_te1550_1*). The loop mirror is made up of a

y-branch splitter and a length of waveguide that connects the two outputs. The Michelson shown in Figure 7 has an optical waveguide length difference of 50um. This should correspond to a FSR of ~5.7nm, similar to an unbalanced MZI with 100um length difference. The output of the Michelson interferometer structure is shown in Figure 8. A sinusoidal response is seen in Figure 8 (blue line) which is similar to the MZI response and the FSR at 1550nm is indeed close to 5.7nm (green dots).

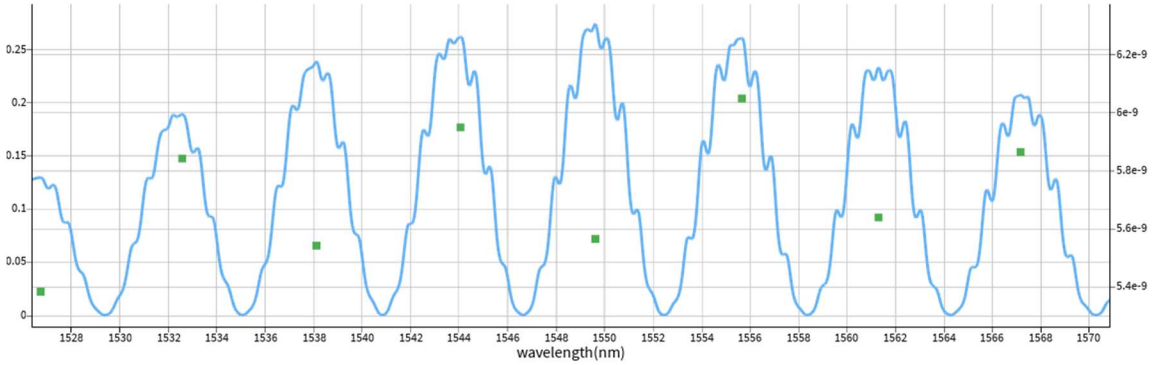

Figure 8: Transmission of an unbalanced Michelson interferometer

4. Fabrication

Figure 9 shows the final mask of the silicon integrated circuit that contains the designs discussed in this report. Included are five length variations of an unbalanced MZI (25-125um) and one length variations of an unbalanced Michelson interferometer (50um). Also included are two calibration structures, one for the MZI and one for the Michelson. These calibration structures will be used to remove the losses associated with the grating couplers and other common components. The total size of the chip is 605um x 410um.

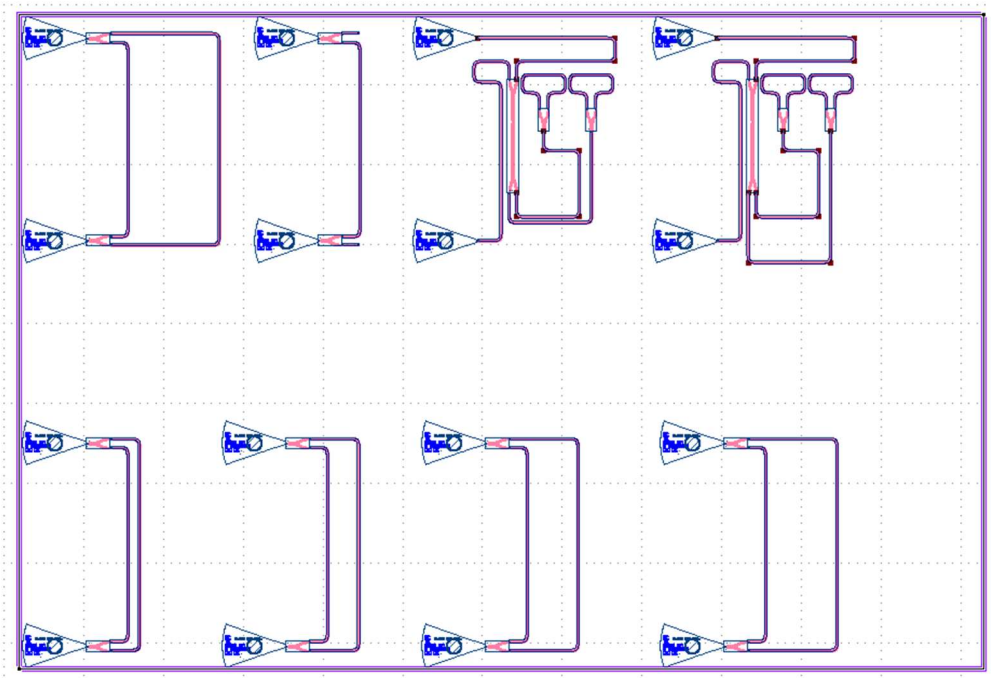

Figure 9: Mask layout of silicon integrated circuit

5. Experimental Data

The mask in Figure 9 was fabricated at Applied Nanotools in Canada using an E-beam process [2]. The structures were measured at the University of British Columbia [1,3,4]. Figure 10 shows the responses of the various MZI's overlayed in a single plot.

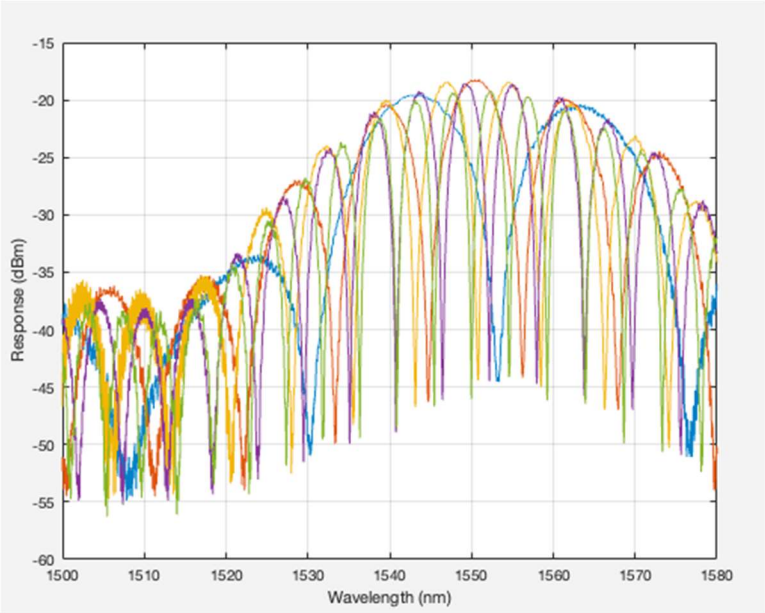

Figure 10: Plot of all five MZI responses

In Figure 10, multiple interference patterns can be seen due to each MZI having a different length offset between their arms. The bandpass nature of the all of the responses is dictated by the grating coupler which appears to have roughly 30nm of bandwidth (1535nm to 1565nm).

Figure 11 shows the response of the unbalanced Michelson interferometer overlayed with the MZI that has the same length offset. There is a slight wavelength shift in the responses of the two interferometers but the period and FSR is the same. It also appears as though the MZI has slightly better insertion loss than the Michelson.

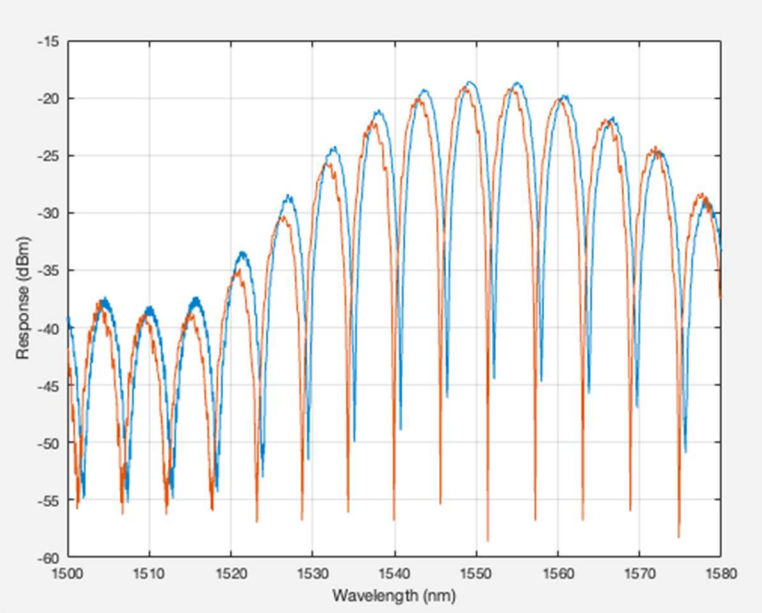

Figure 11: Michelson and Mach-Zehnder interferometers with 100um length offset

6. Analysis

As with any fabrication process, the E-beam method has tolerances on how accurately it can reproduce the structures provided in the mask. While the optical waveguides in this project were all nominally 220nm thick by 500nm wide, the actual realized waveguide width and height depends on many factors. The range of width and height is the tolerance of the process and is shown in Figure 12.

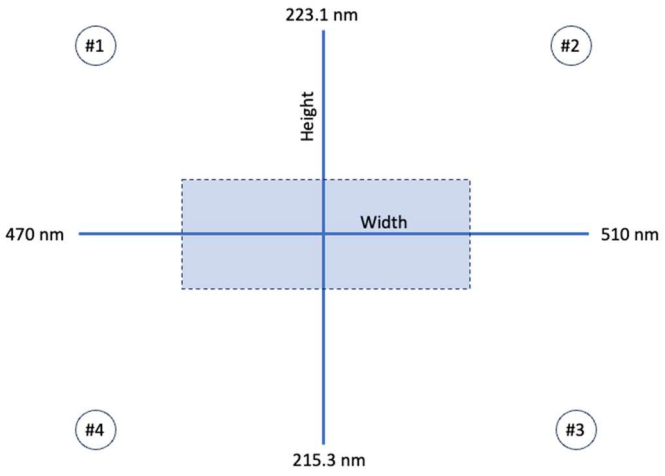

Figure 12: Expected fabrication tolerance of the E-beam process

Figure 12 shows that the width is expected to fall within the range 470nm-510nm and the height is expected to be within 215.3nm and 223.1nm. A tolerance analysis can be completed using the box method. In this method, the four corners of the width and height tolerance (labeled 1-

4 in Figure 12) can be used in simulation to predict circuit performance. In this project, the four corners will be used to predict the group index range of the waveguides in our unbalanced interferometers.

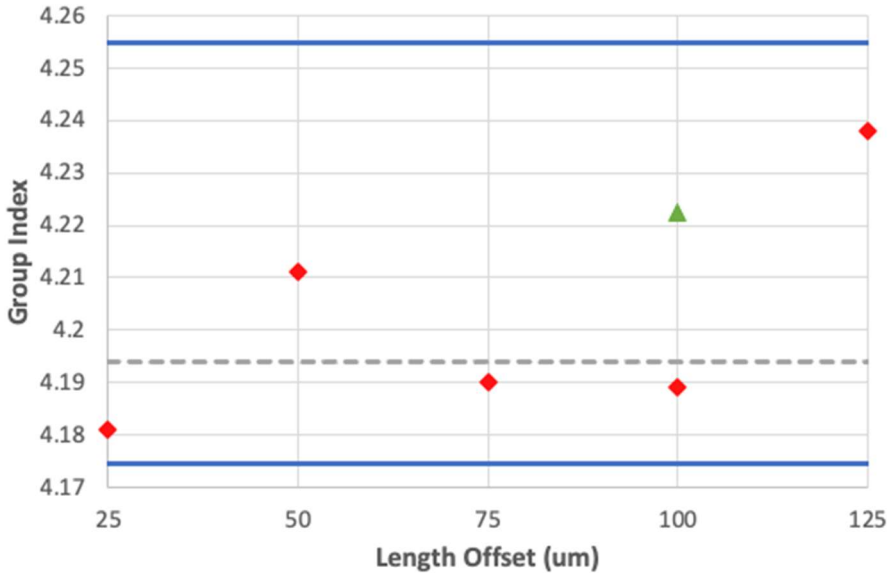

Figure 13: Simulated tolerance bounds of group index and extracted group index form the measured data

Figure 13 shows the simulated tolerance bounds on the group index (blue lines) along with the values obtained through analysis of the MZI experimental data (red diamonds) and Michelson experimental data (green triangle). The ideal group index using a 220nm by 500nm waveguide geometry is shown as a gray dotted line. The group index was found by first extracting the FSR of the various interferometers. This was done by locating the nulls in the interferometer waveform and subtracting adjacent values closest to 1550nm. The FSR was then used in Eq. 4 to find the group index. The experimental points in red and green are well contained within the tolerances predicted in simulation.

7. Conclusion

This report describes the theory, design, and fabrication of a range of unbalanced Mach-Zehnder interferometers on a silicon photonic integrated circuit process. The goal was to extract the optical waveguide group index from the interferometer experimental results and compare it to the value obtained from simulation results. A tolerance analysis was performed to determine what group index variation to expect from the fabrication process. The calculated group index values fell within the expected fabrication tolerance.

References

1. L. Chrostowski and M. Hochberg, *Silicon Photonics Design, Cambridge, UK:* Cambridge University Press, 2015.
2. http://www.appliednt.com/nanosoi, Applied Nanotools, Edmonton, Canada
3. http://siepic.ubc.ca/probestation (using Python code developed by Michael Caverley)
4. http://mapleleafphotonics.com, Maple Leaf Photonics, Seattle WA, USA